JOURNAL OF GEOPHYSICAL RESEARCH, VOL. 85, NO. A13, PAGES 7642-7650, DECEMBER 30, 1980

# An Empirical Model of the Venusian Outer Environment 1. The Shape of the Dayside Solar Wind-Atmosphere Interface

O. L. VAISBERG

*Space Research Institute, USSR Academy of Sciences, Moscow, USSR*

D. S. INTRILIGATOR

*Department of Physics, University of Southern California, Los Angeles, California 90007*

V. N. SMIRNOV

*Space Research Institute, USSR Academy of Sciences, Moscow, USSR*

Solar wind plasma and magnetic field data and ionospheric data obtained from the Pioneer Venus orbiter are considered. It is shown that the variation of the magnetic field pressure within the magnetic barrier is similar to that expected for the solar wind pressure variations along an obstacle's boundary when a more realistic approximation of the shape of the ionosphere is included. Simultaneous solar wind pressure, ionospheric pressure, and magnetic barrier pressure data show that the ionospheric pressure below the ionopause is approximately equal to the solar wind pressure. The magnetic barrier pressure is equal to approximately 2/3 to 3/4 of both the solar wind pressure and the ionopsheric pressure. Estimates of the hot plasma pressure contribution to the total pressure within the magnetic barrier vary from 1/4 to 1/3. Just below the ionopause the ionospheric pressure deviations from the mean ionospheric pressure are significant especially below ~400 km and appear to be indicative of the adjustment of the ionospheric structure to changing solar wind conditions. A first-order model of the ionopause pressure variations as a function of height and solar-zenith angle is suggested. This model provides an estimate of an 'instant' ionopause profile for the given solar wind conditions. The mean and 'instant' shapes of the ionopause do not appear to correspond to the estimates obtained from ionospheric pressure equilibrium for a given $H/r_0$.

## INTRODUCTION

The first measurements near Venus of the magnetic field and plasma revealed that the planetary magnetic field is too weak to prevent the direct interaction of the solar wind plasma with the Venusian atmosphere [*Smith et al.*, 1965; *Dolginov et al.*, 1968]. The existence of a bow shock demonstrated that most of the oncoming solar wind plasma is deflected by the atmosphere of the planet. Several models of the interaction have been proposed [*Johnson and Midgley*, 1969; *Cloutier et al.*, 1969; *Michel*, 1971; *Wallis*, 1972].

Previous data on the height of the Venusian ionopause were obtained by radio occultation from the Mariner 5 and Mariner 10 flyby's [*Fjeldbo et al.*, 1969; *Howard et al.*, 1974] and from the Venera 9 and Venera 10 orbiters [*Ivanov-Kholodnyi et al.*, 1977, 1978] as well as from measurements of the location of the boundary just beyond the terminator [*Romanov et al.*, 1978]. The results of *Romanov et al.* [1978] on the height of the ionopause near the terminator give the ionopause as it was understood in the gas dynamic concept [*Sprieter et al.*, 1970]; i.e., as the lower boundary of an external flow. Recent results from the Pioneer Venus orbiter (PVO) indicate [*Intriligator et al.*, 1979; *Spenner et al.*, 1979] that there is a gap between the ionopause as defined by the upper boundary of the topside ionosphere and the ionopause as defined by the lower boundary of an external flow. A consistent result was obtained by *Vaisberg et al.* [1976], who reported a low-energy plasma population in the tail just behind the terminator (internal flow). Several attempts were made to infer the subsolar ionopause altitude from the shape and location of the bow shock [e.g., *Gringauz et al.*, 1976; *Vaisberg et al.*, 1976; *Russell*, 1977; *Slavin et al.*, 1979]. Recently, the Pioneer Venus orbiter has made detailed measurements of the solar wind plasma interaction and the structure of the Venusian ionosphere and atmosphere [*Science, 203*, No. 4382, 1979; *Science, 205*, No. 4401, 1979].

The Pioneer Venus orbiter data analyses lead to two important conclusions from the point of view of the solar wind interaction with the planet:

1. Above 200 km, the dayside ionosphere is in a state of diffusive equilibrium with the $O^+$ ion as the main constituent. The elevated electron and ion temperatures in the ionosphere together with the number density below the ionopause provide enough pressure, in most cases, to sustain the external solar wind pressure. The height of the ionopause is strongly influenced by the solar wind pressure [*Bauer et al.*, 1979; *Kliore et al.*, 1979*a*; *Knudsen et al.*, 1979*a*; *Taylor et al.*, 1979*a*, *b*].

2. The magnetic field inside the ionosphere is too weak, in most cases, to make a significant contribution to the pressure below the ionopause. Above the ionopause there is a region of increased magnetic field where the magnetic field pressure approximately equals the solar wind pressure. This region of increased magnetic field presumably transfers solar wind pressure to the ionosphere [*Russell et al.*, 1979*a*, *b*; *Knudsen et al.*, 1979*a*; *Brace et al.*, 1979*a*; *Elphic et al.*, 1979]. It seems appropriate to call this region the 'magnetic barrier' because of its similarity to the earlier proposed model [*Michel*, 1971].

Recently, a model of the ionosphere of Venus was proposed in order to explain the variations in the height of the ionopause as determined from radio occultation data in response to changes in the solar wind pressure [*Wolff et al.*, 1979]. Vari-



Paper number 80A1141.
0148-0227/80/080A-1141$01.00

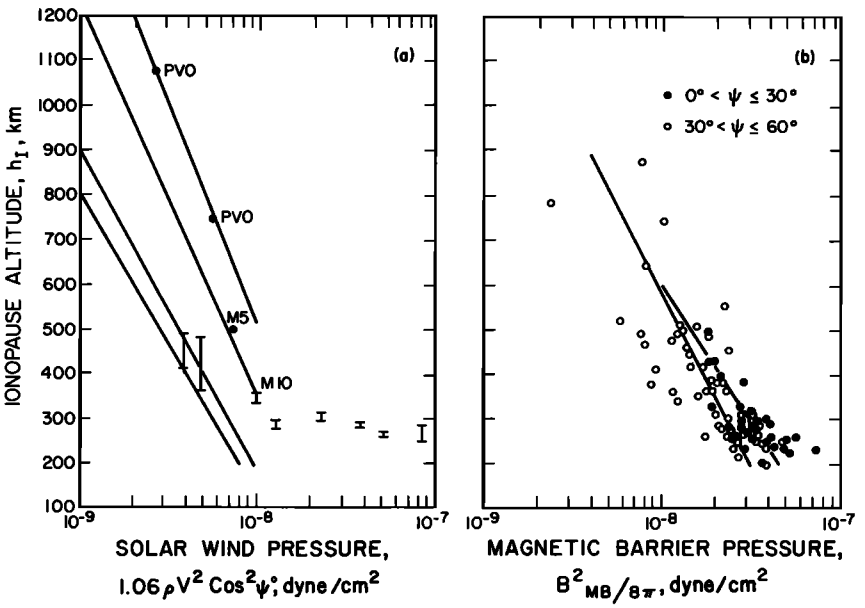


Fig. 1. (*a*) Dayside ionopause altitudes as observed by the radio occultation experiments versus estimated solar wind pressure according to *Wolff et al.* [1979]. The altitudes were measured by Mariner 5, Mariner 10, Pioneer Venus orbiter (PVO), and Venera 9 and Venera 10 (the 7 other crossings). The low-altitude ionopause crossings from Venera 9 and Venera 10 do not fit the model (straight lines) developed by *Wolff et al.* [1979]. (*b*) The height of the ionopause versus magnetic barrier pressure as obtained with the PVO magnetometer data for the solar zenith angle range 0–30° (closed circles) and 30–60° (open circles) [*Elphic et al.*, 1979].

ations in the altitude of the ionopause location above ~400 km were satisfactorily explained by the model that takes into account the effect of variable solar EUV, but large discrepancies between the model and observations of the ionopause were found in the altitude range of 250 to 350 km. Figure 1 summarizes the earlier results on the ionopause altitude variations as a function of the solar wind pressure [*Wolff et al.*, 1979] and as a function of the magnetic barrier pressure [*Elphic et al.*, 1979].

The purpose of this paper is to consider the available data on the ionosphere and magnetic barrier and compare them with solar wind measurements performed on the same spacecraft [*Wolfe et al.*, 1979; *Intriligator et al.*, 1979], in order to make more quantitative estimates of the pressure balance. In addition, we will present a tentative empirical model of the dayside Venusian interaction with the solar wind.

## Pressure Distribution Along the Ionopause

Joint data on the solar wind, magnetic field, and ionosphere are available only for the first period of Pioneer Venus orbiter (PVO) observations in December 1978. Upon insertion into orbit, the solar zenith angle of periapsis of PVO was 61.4°, and periapsis was displaced by ~1.5° toward the nightside on each successive orbit [*Colin*, 1979]. Therefore we are restricted here to solar zenith angles (SZA) >63° for data on the ionosphere and on the near-planetary magnetic field that can be considered in comparison with the solar wind data.

Figure 2 shows the behavior with SZA of the magnetic barrier pressure (determined from the peak magnetic field), according to the data of *Russell et al.*, [1979*a*, *b*] and *Elphic et al.* [1979]. The mean values and the standard deviations of the pressures within the magnetic barrier are shown along with the individual measurements for several orbits where the solar wind data are available. Curve 1 in Figure 2 shows the $\cos^2\psi°$ dependence, where $\psi°$ is the SZA. This dependence is frequently accepted as representing the solar wind pressure change along the ionopause. To fit the low SZA data, this curve was normalized to the subsolar magnetic barrier pressure of ~$3.7 \times 10^{-8}$ dynes/cm$^2$. It is clear from Figure 2 that at large SZA's there is a significant discrepancy between the observed mean pressures and the $\cos^2\psi°$ curve.

The slower change of the external pressure as a function of $\psi°$ compared with the $\cos^2\psi°$ dependence is confirmed by the individual magnetic pressure measurements at larger SZA. To

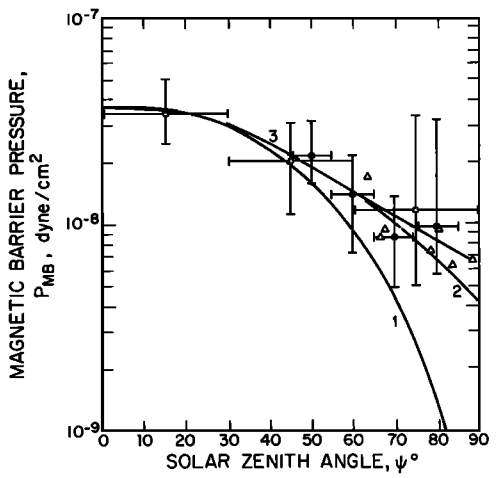


Fig. 2. The dependence on solar zenith angle of the magnetic field pressure in the magnetic barrier region. Closed circles are from *Russell et al.* [1979*b*], open circles are from *Elphic et al.* [1979]. Triangles are the values of the magnetic field pressure for orbits with available solar wind data normalized to the solar wind pressure of $5.2 \times 10^{-8}$ dynes/cm$^2$. Curve 1 is $\cos^2\psi°$; curve 2 is $\cos^2\chi°$ with $\chi$ equal to the expected angle between the normal to the ionopause and the solar wind flow direction; and curve 3 is the gas dynamic pressure variation along the boundary [*Spreiter et al.*, 1968]. The curves are normalized to the subsolar magnetic pressure value of $3.7 \times 10^{-8}$dynes/cm$^2$.

TABLE 1. PVO Solar Wind, Magnetic, and Ionospheric Data Related to the Dayside Ionopause

| Orbit | Day, 1978 | SZA, $\psi°$ | $h_I$, km | $P_{SW_0}$ | $P_\psi$ | $P_{MB}$ | $nk(T_e + T_i)$ | $B_I^2/8\pi$ | $P_I$ |
|---|---|---|---|---|---|---|---|---|---|
| 1 | Dec. 5 | 63.3 | 530 | 4.3 | 1.5 | 1.5 | 1.4 | ≥0.6 | ≤2.0 |
| 2 | Dec. 6 | 64.9 | 830 | | | 0.62 | 1.1 | | 1.1 |
| 3 | Dec. 7 | 66.2 | 460–570 | 5.6 | 1.8 | 0.92 | 1.3 | <0.004 | 1.3 |
| 4 | Dec. 8 | 67.8 | 930–1080 | 2.1 | 0.65 | 0.41 | 0.72 | <0.002 | 0.72 |
| 5 | Dec. 9 | 69.4 | 1700–1750 | | | | 0.14 | | ≥0.14 |
| 6 | Dec. 10 | 71.0 | 750 | 3.8 | 1.07 | | | | |
| 9 | Dec. 13 | 75.7 | 280–360 | 15.9 | 4.0 | | 4.9 | | ≥4.9 |
| 11 | Dec. 15 | 78.8 | | 23.6 | 5.2 | 3.6 | | 0.92 | |
| 12 | Dec. 16 | 80.3 | >400 | 2.4 | 0.52 | 0.46 | <1.0 | <0.004 | <1.0 |
| 14 | Dec. 18 | 83.5 | | 8.5 | 1.7 | 1.1 | | 0.06–0.16 | |
| 17 | Dec. 21 | 88.2 | | 4.9 | 0.85 | ~0.66 | | <0.05 | |
| 18 | Dec. 22 | 89.8 | 450–500 | | | 0.3–0.9 | 0.48 | 0.006 | ≤0.48 |

All pressures are given in units of $10^{-8}$ dynes/cm$^2$.

allow for day-to-day solar wind pressure changes, the magnetic barrier pressures were normalized to the free stream solar wind pressures observed on the same orbits. The mean solar wind pressure chosen to normalize the data was taken = 1.4 × (the subsolar magnetic pressure) = 1.4 × ($3.7 \times 10^{-8}$ dynes/cm$^2$) = $5.2 \times 10^{-8}$ dynes/cm$^2$. The factor 1.4 takes into consideration the pressure of the hot plasma inside the magnetic barrier. This factor will be discussed in detail later. It is seen from Figure 2 that with the data (normalized in this way) there is a good fit to the distribution of the mean magnetic barrier pressure. Also, the figure shows that this variation with SZA is not as large as the $\text{Cos}^2\ \psi°$.

A major part of the discrepancy between the observed pressure variations and the $\text{Cos}^2\ \psi°$ dependencies is associated with the deviation of the ionopause from a spherical surface. To obtain an estimate of the external pressure variation with SZA, we assumed that the surface of the ionopause can be obtained from a simple ionospheric pressure balance [*Spreiter et al.*, 1970] with $H/r_0 = 0.07$ [*Knudsen et al.*, 1979*a*], where $H$ is the ionospheric scale height and $r_0$ is the planetocentric subsolar dimension of the obstacle. This assumption considerably improves the agreement between the expected and observed change of the magnetic barrier pressure with SZA as shown by curve 2 in Figure 2.

Further improvement can be obtained by taking into account the deviation of the gas dynamic pressure from a simple $\text{Cos}^2\ \psi°$ law for large $\psi°$ angles [*Spreiter et al.*, 1968]. Curve 3 in Figure 2 shows this gas dynamic pressure distribution. The variation of the mean magnetic pressure within the magnetic barrier shown by curve 3 in Figure 2 can be approximated by the equation:

$$P_{MB} = 3.7 \times 10^{-8}\ \text{Cos}^2\ (\psi° - 0.00275\psi°^2)\ \text{dynes/cm}^2 \quad (1)$$

These results confirm the supposition that the pressure within the magnetic barrier is determined by the solar wind pressure [*Russell et al.*, 1979*a*, *b*; *Elphic et al.*, 1979] and shows that this supposition holds for SZA's up to ~90°. In subsequent considerations we will use the gas dynamic pressure distribution (curve 3, Figure 2).

## Pressure Balance Across the Ionopause

Table 1 summarizes all the available data on the solar wind, ionosphere, and magnetic field for the first period of PVO observations when the periapsis of the orbiter was on the dayside of Venus. The solar wind data are from the PVO plasma analyzer [*Wolfe et al.*, 1979; *Intriligator et al.*, 1979]. All other data were taken from other publications and the figures therein [*Bauer et al.*, 1979; *Brace et al.*, 1979*a*, *b*; *Cravens et al.*, 1979; *Elphic et al.*, 1979; *Knudsen et al.*, 1979*a*, *b*; *Nagy et al.*, 1979; *Russell et al.*, 1979*a*, *b*; *Taylor et al.*, 1979*a*, *b*). Since most of the published data do not have detailed orbital information all the data were attributed to the SZA for periapsis ($\psi_\pi$) of the respective orbit.

In most cases for large SZA, the SZA for the PVO ionopause crossing is within ~3° of $\psi_\pi$. The resulting errors, therefore, are not expected to be large since the change of the external pressure with SZA (i.e., curve 3 in Figure 2) is much less than $\text{Cos}^2\ \psi$. For the cases when the measurements were available for both the inbound and outbound parts of the orbit, the data were averaged.

The ionopause altitudes, $h_T$, were also taken from the tables and/or figures in the respective publications. The free stream solar wind pressure, $P_{SWO}$, was calculated from the data of the PVO plasma analyzer by using the formula $P_{SWO} = 1.06\ \rho V^2$. $V$ is the solar wind speed and $\rho$ is the proton mass density. An aerodynamic factor of 0.881 for flow in this range of solar zenith angles is derived from *Spreiter et al.* [1970], and an assumed $He^{++}$ number abundance of 5% increases the mass density by 20%. The product of these two corrections gives the factor of 1.06. The pressure on the ionopause at SZA $\psi$, $P_\psi$, is obtained from $P_{SWO}$ by using (1). The magnetic pressure within the magnetic barrier, $P_{MB} = B_{MB}^2/8\pi$, was obtained from the peak field values. The ionospheric pressure, $nk(T_e + T_i)$, was obtained from the ionospheric number density ($n$) taken just below the ionopause and from the mean distributions of the ion and electron temperatures ($T_i$ and $T_e$) with height (as discussed in more detail below). The magnetic pressure within the ionosphere, $B_I^2/8\pi$, was taken into account in calculating the total ionospheric pressure $P_I$. The large magnetic field 'inclusions' reported by *Russell et al.* [1979*b*] may have been recorded as a result of the spacecraft's repeated passes near the lower edge of the magnetic barrier due to the specific SZA profile of the ionopause (see below). If this supposition is correct, the addition of the magnetic term in the total pressure within the ionosphere should be made with caution.

The comparison of the solar wind, magnetic barrier, and ionospheric pressures are given in Figure 3. In Figure 3 the arrows indicate the contribution of the ionospheric magnetic field. Taking into account the uncertainties connected with measurement errors, data processing, and temporal variations due to possible changes in the solar wind conditions during

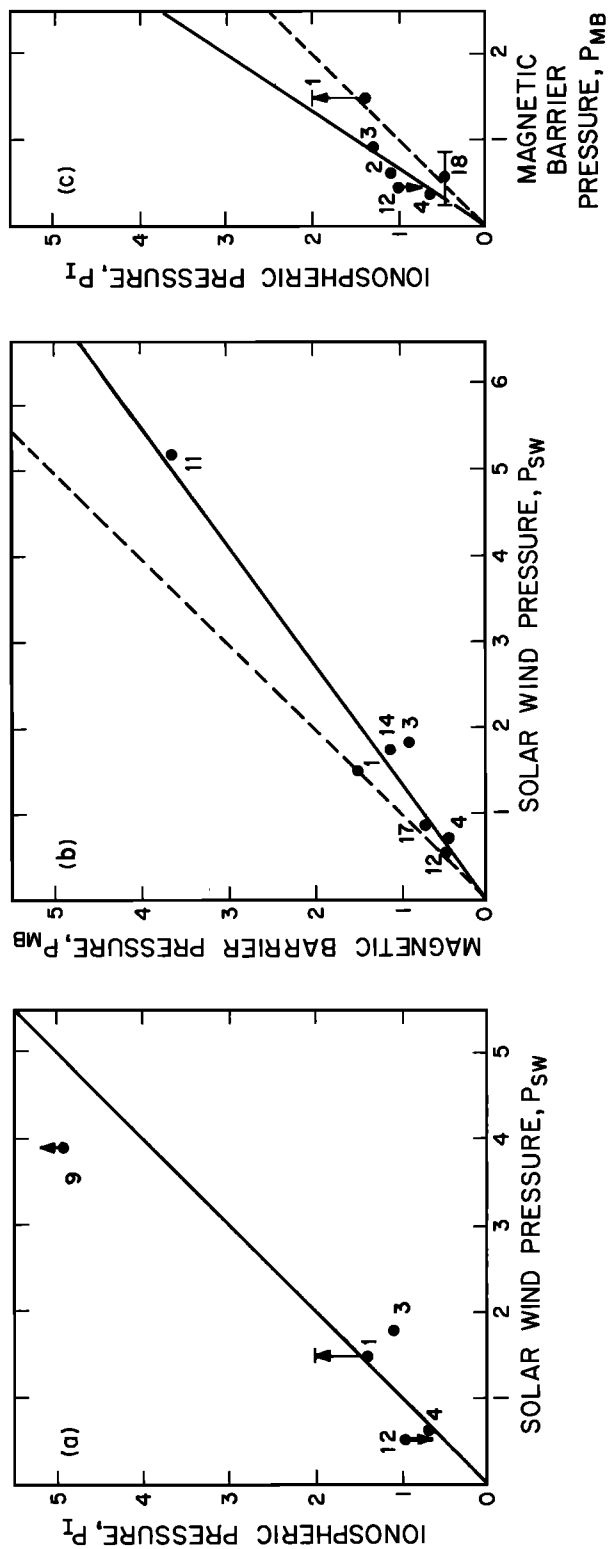


Fig. 3. Comparison of measured PVO pressure values. (*a*) Ionospheric pressure versus solar wind pressure. (*b*) Magnetic barrier magnetic pressure versus solar wind pressure. (*c*) Ionospheric pressure versus magnetic barrier magnetic pressure. Units are $10^{-8}$dyne/cm$^2$. Orbit numbers are indicated (see Table 1). The pressure increase in the ionosphere due to the ionospheric magnetic field is indicated by the arrow for orbit 1, and the lack of magnetic field data for orbit 9 may affect the value of the ionospheric pressure. The upper limit for the ionospheric pressure is indicated for orbit 12. Straight lines are drawn to fit the data. Dashed lines on panels (*b*) and (*c*) indicate the expected direct proportionality between the respective pressures.

the spacecraft's pass within the interior region, it appears that the agreement between the solar wind pressure (calculated from the free stream $\rho V^2$ value with SZA variations according to gas dynamic analogy [*Spreiter et al.*, 1968]) and the ionospheric pressure is reasonable (the mean ratio of $P_\psi/P_I = 0.96 \pm 0.29$). There appears to be a systematic deviation of the magnetic barrier pressure $B_{MB}^2/8\pi$ from both the solar wind pressure and the ionospheric pressure. The mean ratio of the magnetic barrier pressure to the solar wind pressure is $0.73 \pm 0.15$ (where 0.15 is the standard deviation) and the mean ratio of the magnetic barrier pressure to the ionospheric pressure is $0.65 \pm 0.10$. This most likely implies that although the magnetic barrier pressure plays a major role in the transfer of solar wind pressure to the ionosphere the plasma pressure within the magnetic barrier may provide an additional pressure equal to about 1/4 to 1/3 of the total pressure. This contribution from the plasma seems indirectly confirmed when one compares the magnetic and ionospheric pressure variations across the ionopause (see Figure 1 in *Elphic et al.* [1979]). The magnetic pressure within the magnetic barrier was about $1.3 \times 10^{-8}$ dynes/cm$^2$. The sum of the total pressure and the ionospheric plasma pressure within the ionopause, $(B_I^2/8\pi + nk(T_e + T_i))$, was almost equal to the ionospheric plasma pressure below the ionopause and was about $1.6 \times 10^{-8}$ dynes/cm$^2$. These numbers indicate that the pressure jumps across the ionopause by a factor of ~1.25 and that there is a possible contribution from the hot plasma to the magnetic pressure.

The existence of a magnetic barrier region containing a small amount of hot plasma can be considered in terms of a depletion layer as first suggested by *Zwan and Wolf* [1976].

Our estimate for the mean contribution of the plasma pressure to the total magnetic barrier pressure is on the order of a few tenths. The relative role of the plasma and the magnetic field in the layer above the ionopause may change depending on many parameters, including the SZA, the angle between the magnetic field vector, and the flow velocity vector, etc. It is anticipated that eventually more detailed information can be obtained from the PVO OIMS data as well as from continuing analyses of the PVO plasma analyzer data.

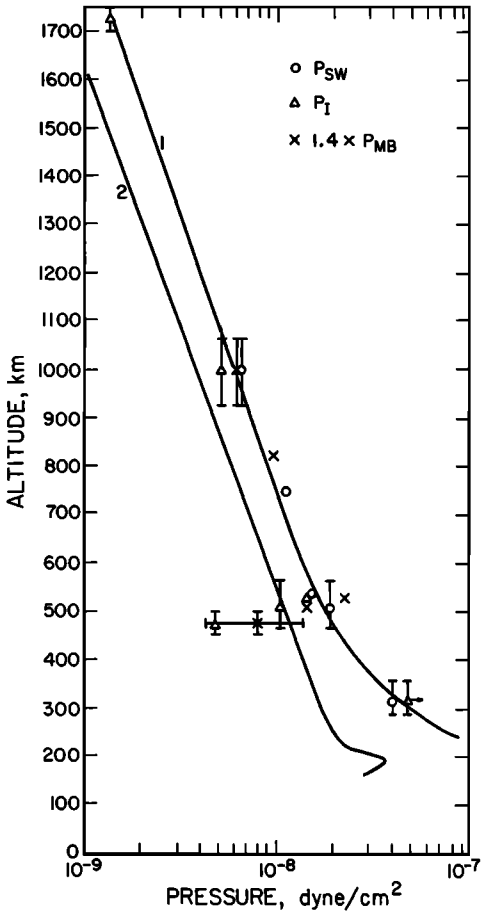


Fig. 4. The solar wind pressure, the magnetic barrier pressure increased by a factor of 1.4, and the total (kinetic and magnetic) pressure of the ionosphere below the ionopause plotted against the observed ionopause altitudes for the first orbits of PVO. Curve 1 is drawn to show the change of pressure values at the ionopause with altitude for the SZA range 65–75°. The mean ionospheric pressure model (curve 2) is shown for comparison (see text).

## THE SHAPE OF THE IONOPAUSE

Curve 1 in Figure 4 shows how the subionopause pressure (i.e., the pressure just below the ionopause) varies with altitude for large SZA (~70°). This curve was obtained by connecting the pressure values indicated in the figure. We have included the pressure contribution from the hot plasma in the total magnetic barrier pressure. This figure demonstrates once again the fair agreement between the solar wind, ionospheric and magnetic barrier pressure data.

An empirical model of the mean ionospheric plasma pressure distribution $nk(T_e + T_i)$, for the same period of observations and the same range of SZA is shown by curve 2 in Figure 4. A number of assumptions were made in obtaining curve 2:

1. A mean profile of the ionospheric number density was adopted. Below 500 km the number density falls within the middle of the range of the retarding potential analyzer measurements [*Knudsen et al.*, 1979*a*]. Above 500 km the ionospheric density is proportional to the $O^+$ number density measurements on the fifth PVO orbit when the ionopause height was at 1750 km [*Taylor et al.*, 1979*a*, *b*].

2. The electron temperature profile was adopted from the electron temperature probe measurements on the fourth orbit of PVO up to ~950 km [*Knudsen et al.*, 1979*b*], and above this height $T_e$ was taken to be equal to 5500°K.

3. The ion temperature profile was chosen to be in the middle of the range of the measured temperatures up to ~500 km [*Knudsen et al.*, 1979*b*]. Between 500 km and 950 km it was taken as proportional to $T_e$ ($T_i = 0.4T_e$), and above this altitude it was taken as 2600°K.

It can be seen from Figure 4 that, calculated in this way, the ionospheric pressure is proportional to the subionopause pressure distribution for heights above approximately 400 km and that the pressure versus altitude dependence does not follow the ionospheric pressure distribution for the lower altitude range. The behavior of this simple model for the lower ionopause heights is in good agreement with the results of *Wolff et al.* [1979]. The subionopause pressure never equals the mean ionospheric pressure distribution in any altitude range, a result which seems significant and will be discussed later.

The data in Figure 4 give us some foundation to use a simple model of the subionopause pressure to estimate the location and shape of the ionopause for different solar wind conditions. Since we have considered so far only the region of large SZA, it is necessary to allow for a possible change of ionospheric conditions with SZA.

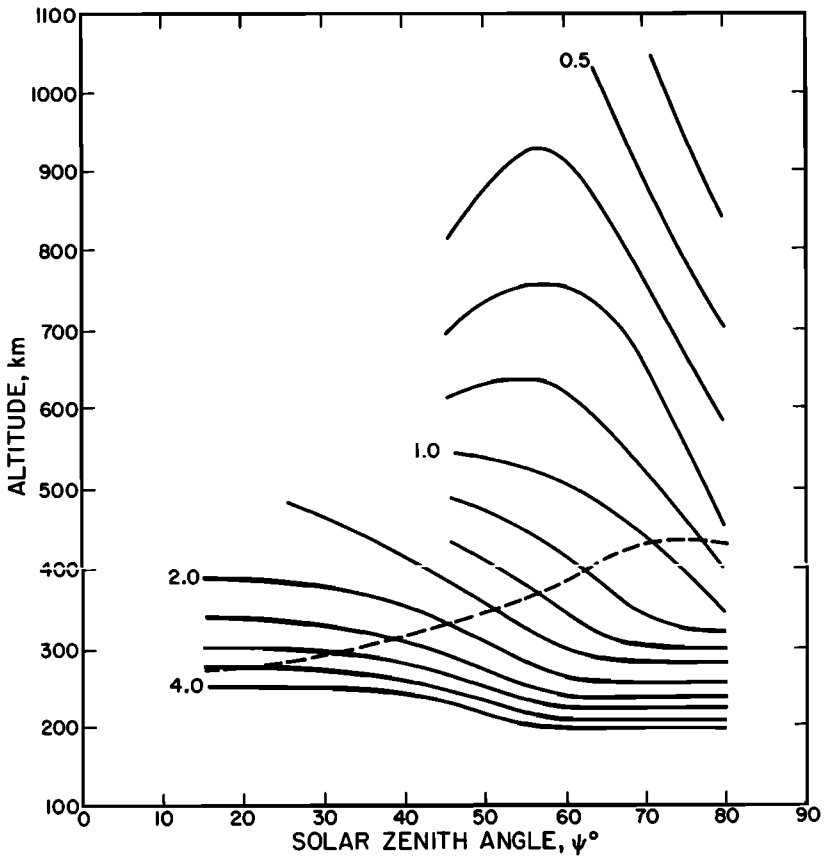


Fig. 5. The solid contour lines show the median magnetic barrier pressure as a function of altitude and SZA as suggested by the magnetic field measurements [*Russell et al.*, 1979*b*; *Elphic et al.*, 1979]. Contour labels are pressures in units of $10^{-8}$ dynes/cm$^2$. The dashed line shows the expected ionopause location for the approximate mean solar wind pressure.

The most extensive data set on the ionopause locations and on the magnetic pressure within the magnetic barrier were published by *Russell et al.* [1979*a*] and *Elphic et al.* [1979]. These results indicate that conditions near the ionopause change with solar zenith angle. We have used the data of *Russell et al.* [1979*b*] and *Elphic et al.* [1979] to reconstruct the near-ionopause magnetic pressure changes with altitude and SZA. This reconstruction was made graphically by drawing smooth lines through the individual magnetic pressure values obtained from averaging the observed magnetic pressures versus ionopause altitudes for the various SZA intervals given by *Russell et al.* [1979*b*] and *Elphic et al.* [1979]. The resulting pressure distribution is shown in Figure 5. No allowance has been made for the possible dawn-dusk asymmetry of the ionospheric and magnetic field conditions, which is suggested by recent measurements [*Taylor et al.*, 1979*a*, *b*; *Elphic et al.*, 1979]. It should be noted that in Figure 5 the value of the near-ionopause magnetic pressure is not the mean value but rather the median magnetic pressure that implies a slightly smaller value for the pressure due to the nonsymmetric distribution of the observed pressure values around the mean.

The mean magnetic pressure distribution versus SZA ($\psi$) and ionopause height ($h_I$) can be approximated by the equation

$$P_{MB} = P_\psi^{(1)} e^{-h_I/H_1} + P_\psi^{(2)} e^{-h_I/H_2} \quad (2)$$

The form of (2) was suggested by the shape of the $P_{MB}/h_I$ dependencies published by *Russell et al.* [1979*b*] and *Elphic et al.* [1979]. A reasonable fit to the observed points was obtained with $P_\psi^{(1)} = (130 - 0.045\psi - 0.009\psi^2) \times 10^{-8}$, $P_\psi^{(2)} = (3.5 - 0.009\psi - 0.00025\psi^2) \times 10^{-8}$, $H_1 = 60$, $H_2 = 700$, where the pressures are in dynes/cm$^2$, $\psi$ is in degrees, and the heights are in kilometers.

Taking into account the aerodynamic pressure change with SZA and assuming that the magnetic pressure above the ionopause is approximately 2/3 of the total pressure at all SZA, we can obtain the trace of the ionopause on the pressure distribution for a given solar wind pressure. An example of such an ionopause trace is shown in Figure 5, which corresponds to an observed mean subsolar magnetic pressure within the magnetic barrier equal to $3.7 \times 10^{-8}$ dynes/cm$^2$. This ionopause profile represents conditions close to the mean for the time interval under discussion.

Figure 6 displays all the published data on the ionopause altitudes versus SZA [*Fjeldbo et al.*, 1969; *Howard et al.*, 1974; *Romanov et al.*, 1978; *Ivanov-Kholodnyi et al.*, 1977, 1978; *Brace et al.*, 1979*a*; *Kliore et al.*, 1979*a*, *b*; *Knudsen et al.*, 1979*a*; *Taylor et al.*, 1979*a*, *b*]. All available data were employed, and some crossings may appear two or three times, if they are described in the published data for more than one experiment.

Three 'snapshots' of the ionopause profile are shown: the middle profile corresponds approximately to the mean solar wind conditions and the profiles above it and below it, respectively, correspond to changes of the solar wind pressure by factors of 0.5 and 2, respectively. These factors correspond to the mean square variations of the solar wind number density [*Diodato et al.*, 1974]. Since we do not know the mean value of

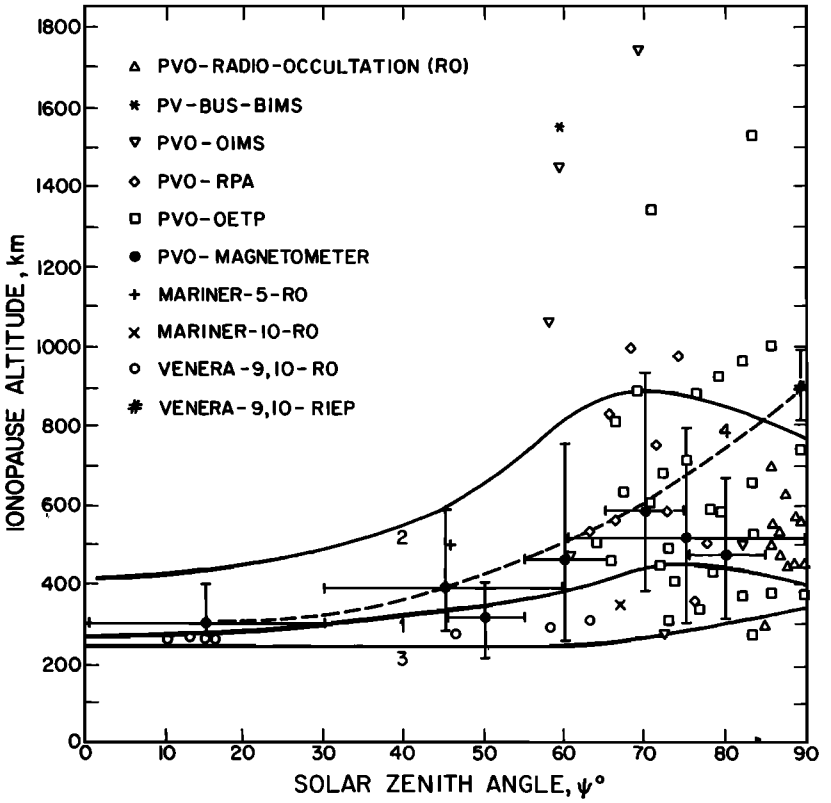


Fig. 6. The observed ionopause altitudes versus solar zenith angle. The expected 'instant' ionopause profiles are shown for the approximate mean solar wind pressure value (curve 1), one half of it (curve 2), and twice the mean pressure value (curve 3). The dashed line indicates the model ionopause profile for $H/r_0 = 0.07$ and $r_0 = 6350$ km.

the solar wind pressure for the time intervals under consideration, these ionopause profiles do not necessarily represent real ones for mean conditions. Also it should be noted that owing to the nonsymmetric distribution of observed ionopause altitudes an 'instant' profile for the mean solar wind pressure does not correspond to the observed mean ionopause heights for different SZA's. It can be seen from Figure 6, however, that the 'instant' profiles reasonably represent the distribution of the observed ionopause crossings.

## Discussion

The ionopause profiles obtained do not follow a simple hydrostatic equilibrium model of the ionosphere (shown here for $H/r_0 = 0.07$ and $r_0 = 6350$ km). The observed distribution of the ionopause crossings [*Ivanov-Kholodnyi et al.*, 1977, 1978; *Russell et al.*, 1979*b*; *Elphic et al.*, 1979] shows that almost no ionopause crossings have been observed below 200 km and that the locations of the ionopause in the altitude range of 250–300 km were recorded over a wide range of solar wind pressures. This suggests that the height of ~250 km may be considered as a saturation height that stabilizes the ionopause location over a relatively wide range of solar wind pressures. It was pointed out by *Wolff et al.* [1979] that in the altitude range of 250–350 km the slope of the curve of $dh_I/dP_{sw}$ is much less than for higher altitudes. We estimated an 'effective scale height' of ~30 km from their $h_I$, $P_{sw}$ dependence (see Figure 2, *Wolff et al.* [1979] and Figures 1 and 4 in this paper) for the altitude range 250–350 km. This scale height is several times smaller than the ionosphere scale height at these altitudes.

The ionospheric pressure profile for SZA ~70° shows a strong change of the pressure gradient somewhere below 220 km. This fact, along with the significant deviation of the subionopause pressure profile (Figure 4) from the ionospheric pressure profile, shows that the simple consideration of the pressure balance across the ionopause with the use of the mean ionospheric pressure profile cannot explain the observed distribution of ionopause locations.

Several effects may contribute to the stabilizing properties of the Venusian ionopause. The redistribution of ionospheric ionization by increased solar wind pressure was revealed by PVO observations [*Brace et al.*, 1979*a*; *Taylor et al.*, 1979*b*], and a change of the ionospheric number density height profile in the subionopause layer is also suggested by these observations [*Taylor*, 1979*a*, *b*]. Another source that may increase the pressure in the subionopause layer is the rise in the temperature of this layer due to solar wind heating [*Bauer et al.*, 1979; *Brace et al.*, 1979*a*; *Knudsen et al.*, 1979 *a*, *b*; *Scarf et al.*, 1979]. This is confirmed by the height-temperature profile [*Brace et al.*, 1979*a*; *Knudsen et al.*, 1979*b*] and partly by the distribution of the subionopause pressure (Figure 5). Also, the possible influence of the neutral atmosphere on the ionopause properties at lower altitudes should be considered. Ion temperature measurements [*Knudsen et al.*, 1979*b*] show that the maximum in the temperature gradient occurs at a height of ~280 km, which is consistent with significant ion-neutral coupling in this altitude range.

Another major difference between the simple hydrostatic equilibrium model of the ionopause and the observations is evident in Figure 2 for SZA > 70°. The slight decrease of the

ionopause height at SZA > 70° may be real and suggests the existence of a dayside ionospheric bulge. The lower height of the near-terminator ionopause may be connected to significant negative ionospheric density gradients near the terminator [*Brace et al.*, 1979*b*]. The strong ionospheric drifts observed with PVO instrumentation [*Taylor et al.*, 1979*b*] and implied by the 'flat' ionospheric profiles of the near-terminator ionosphere [*Kliore et al.*, 1979*a*] also may significantly contribute to the low ionopause height near the terminator. There is other experimental evidence of ionospheric motions near the terminator [*Taylor et al.*, 1979*b*; *Nagy et al.*, 1979; *Bauer et al.*, 1979]. The important influence of the solar wind drag on ionospheric dynamics was stressed by *Knudsen et al.* [1979*b*], *Perez-de-Tejada and Dryer* [1976], and *Perez-de-Tejada et al.* [1977]. Further analysis of the data and the dynamics of the ionosphere are needed to understand what specific processes of plasma and heat transport are responsible for the existence of a nearly flat or declining ionopause profile near the terminator.

The ionopause profile model obtained above can be used for comparison with hydrodynamic analogy models. The mean ratio of the terminator to subsolar altitudes of the ionopause corresponds to a change in $H/r_0$ from <0.01 to 0.04. Therefore the shape of ionopause that may be used for comparison with aerodynamic model calculations [*Spreiter et al.*, 1970] appears not to correspond to the $H/r_0$ parameter calculated from the ionospheric scale height.

## CONCLUSIONS

First, comparison of simultaneous plasma, magnetic, and ionospheric data confirms previous results that the thermal pressure at the topside ionosphere of Venus balances the external solar wind pressure $\rho V^2$ and that the magnetic barrier formed above the ionopause transfers solar wind pressure to the ionosphere. It is estimated that the hot plasma may contribute approximately from 1/4 to 1/3 of the total pressure within the magnetic barrier region.

Second, the observed ionopause profile does not follow the simple static ionospheric equilibrium model. The dayside ionopause appears to consist of three regions:

1. The low-altitude subsolar region where heating by the solar wind may have a stabilizing effect on the subsolar ionopause height.
2. The region of intermediate solar zenith angles where the height of the ionopause increases with SZA approximately as expected from a simple static equilibrium model.
3. The region near the terminator where there is a 'flat' part of the ionopause that presumably is determined by thermal conditions and by convective ionospheric motions caused by solar wind momentum transfer.

The strong influence of solar wind heating and momentum transfer suggests that the shape and the location of the ionopause may reflect the history of the solar wind-ionosphere interaction. Perhaps a more complicated model should be developed to determine the instantaneous height of the ionopause with better accuracy.

*Acknowledgments.* The authors are indebted to W. David Miller for his participation in the analyses. This work was performed at the University of Southern California. The participation of D. S. Intriligator was supported by NASA contract NAS2-9478.

## REFERENCES

Bauer, S. J., T. M. Donahue, R. E. Hartle, and H. A. Taylor, Jr., Venus ionosphere: Photochemical and thermal diffusion control of ion composition, *Science, 205,* 109, 1979.

Brace, L. H., R. F. Theis, J. P. Krehbiel, A. F. Nagy, T. M. Donahue, M. B. McElroy, and A. Petersen, Electron temperatures and densities in the Venus ionosphere: Pioneer Venus orbiter electron temperature probe results, *Science, 203,* 763, 1979*a*.

Brace, L. M., R. F. Theis, H. B. Niemann, H. G. Mayr, W. R. Hoegy, and A. F. Nagy, Empirical models of the electron temperature and density in the nightside Venus ionosphere, *Science, 205,* 102, 1979*b*.

Cloutier, P. A., M. B. McElroy, and F. C. Michel, Modification of Martian ionosphere by the solar wind, *J. Geophys. Res., 74,* 6215, 1969.

Colin, L., Encounter with Venus, *Science, 203,* 743, 1979.

Cravens, T. E., A. F. Nagy, L. H. Brace, R. H. Chen, and W. C. Knudsen, The energetics of the ionosphere of Venus: A preliminary model based on Pioneer Venus observations, *Geophys. Res. Lett., 6,* 341, 1979.

Diodato, L., G. Moreno, and C. Signorini, Long-term variations of the solar wind proton parameters, *J. Geophys. Res., 79,* 5095, 1974.

Dolginov, Sh. Sh., E. G. Eroshenko, and L. N. Zhuzgov, Magnetic field investigation with spacecraft Venera 4, *Cosmic Res., 6,* 469, 1968.

Elphic, R. C., C. T. Russell, J. A. Slavin, L. H. Brace, and A. F. Nagy, The location of the dayside ionopause of Venus: Pioneer Venus orbiter magnetometer observations, submitted to *Geophys. Res. Lett.*, 1979.

Fjeldbo, G., and V. R. Eshleman, Atmosphere of Venus as studied with the Mariner 5 dual radio frequency occultation experiment, *Radio Sci., 4,* 879, 1969.

Gringauz, K. I., V. V. Bezrukikh, T. K. Breus, T. Gombosi, A. P. Remizov, M. L. Verigin, and G. T. Volkov, Plasma observations near Venus onboard the Venera 9 and 10 satellites by means of wide angle plasma detectors, in *Physics of Solar Planetary Environments,* edited by D. J. Williams, p. 918, AGU, Washington, D. C., 1976.

Howard, H. T., G. L. Tuler, G. Fjeldbo, A. J. Kliore, G. S. Levy, D. L. Brunn, R. Dickinson, R. E. Edelson, W. L. Martin, R. B. Postal, B. Seidal, T. T. Sesplaukis, D. L. Shirley, C. T. Stelzried, D. N. Sweetnam, A. G. Zygielbaum, P. B. Esposito, J. D. Anderson, I. I. Shapiro, and R. D. Reasenberg, Venus: Mass, gravity field, atmosphere, and ionosphere as measured by the Mariner 10 dual-frequency radio system, *Science, 283,* 1297, 1974.

Intriligator, D. S., H. R. Collard, J. D. Mihalov, R. C. Whitten, and J. H. Wolfe, Electron observations and ion flows from the Pioneer Venus orbiter plasma analyzer experiment, *Science, 205,* 116, 1979.

Ivanov-Kholodnyi, G. S., M. A. Kolosov, N. A. Savich, Yu. N. Aleksandrov, M. B. Vasilev, A. S. Vyshlov, V. M. Dubrovin, A. L. Zaitsev, V. A. Samovol, L. N. Samoznaev, A. I. Sidorenko, A. F. Khasyanov, and D. Ya. Shtern, The ionosphere of Venus from the data of the satellites 'Venera 9, 10' and some singularities of its formation, *Sov. Phys. Usp., Engl. Transl., 20,* 1025, 1977.

Ivanov-Kholodnyi, G. S., M. A. Kolosov, N. A. Savich, Yu. N. Alexandrov, M. B. Vasiliev, A. S. Vyshlov, V. M. Dubrovin, A. L. Zaitsev, A. V. Michailov, G. M. Petrov, V. A. Samovol, L. N. Samoznaev, A. I. Sidorenko, and A. F. Hasyanov, Day-time ionosphere of Venus in data of dual-frequency radio occultation experiments with satellites Venera 9, 10, paper presented at 21st meeting of Cospar, Innsbruck, Austria, 1978.

Johnson, F. S., and J. F. Midgley, Induced magnetosphere of Venus, *Space Res., 9,* 760, 1979.

Kliore, A. J., R. Woo, J. W. Armstrong, I. R. Patel, and T. A. Croft, The polar ionosphere of Venus near the terminator from early Pioneer Venus orbiter radio occultations, *Science, 203,* 765, 1979*a*.

Kliore, A. J., I. R. Patel, A. F. Nagy, T. E. Cravens, and T. I. Gombosi, Initial observations of the nightside ionosphere of Venus from Pioneer Venus radio occultations, *Science, 205,* 99, 1979*b*.

Knudsen, W. C., K. Spenner, R. C. Whitten, J. R. Spreiter, K. L. Miller, and V. Novak, Thermal structure and major ion composition of the Venus ionosphere: First RPA results from Venus orbiter, *Science, 203,* 757, 1979*a*.

Knudsen, W. C., K. Spenner, R. C. Whitten, J. R. Spreiter, K. L. Miller, and V. Novak, Thermal structure and energy influx to the day- and nightside Venus ionosphere, *Science, 205,* 105, 1979*b*.

Michel, F. C., Solar wind interaction with planetary atmospheres,

*Rev. Geophys. Space Phys., 9,* 427, 1971.
Nagy, A. F., T. E. Cravens, R. H. Chen, H. A. Taylor, Jr., L. H. Brace, and H. C. Brinton, Comparison of calculated and measured ion densities on the dayside of Venus, *Science, 205,* 107, 1979.
Perez-de-Tejada, H., and M. Dryer, Viscous boundary layer for the Venusian ionosphere, *J. Geophys. Res., 81,* 2023, 1976.
Perez-de-Tejada, H., M. Dryer, and O. L. Vaisberg, Viscous flow in the near-Venusian plasma wake, *J. Geophys. Res., 82,* 2837, 1977.
Romanov, S. A., V. N. Smirnov, and O. L. Vaisberg, On the nature of solar wind-Venus interaction, *Cosmic Res., 16,* 603, 1978.
Russell, C. T., The Venus bow shock: Detached or attached?, *J. Geophys. Res., 82,* 625, 1977.
Russell, C. T., R. C. Elphic, and J. A. Slavin, Initial Pioneer Venus magnetic field results: Dayside observations, *Science, 203,* 745, 1979*a*.
Russell, C. T., R. C. Elphic, and J. A. Slavin, The solar wind interaction with Venus, paper presented at Magnetospheric Boundary Layer Conference, European Space Agency, Alpbach, Austria, Aug. 1979*b*.
Scarf, F. L., W. W. L. Taylor, and J. M. Green, Plasma waves near Venus: Initial observations, *Science, 203,* 748, 1979.
*Science, 203,* 743–808, 1979.
*Science, 205,* 41–121, 1979.
Slavin, J. A., R. C. Elphic, and C. T. Russell, Position and shape of the Venus bow shock: Pioneer Venus orbiter observations, *Geophys. Res. Lett., 6,* 901, 1979.
Smith, E. J., L. Davis, Jr., P. J. Coleman, Jr., and C. P. Sonett, Magnetic measurements near Venus, *J. Geophys. Res., 70,* 1571, 1965.
Spenner, K., W. E. Knudsen, and K. L. Miller, Observations of the Venus ionospheric mantle formed between ionosphere and ionosheath, Report to the IAGA Assembly, Canberra, Australia, 1979.
Spreiter, J. R., A. Y. Alksne, and A. L. Summers, External aerodynamics of the magnetosphere, in *Physics of the Magnetosphere,* edited by R. L. Carovillano, J. F. McClay, and M. R. Radoski, D. Reidel, Hingham, Mass., 1968.
Spreiter, J. R., A. L. Summers, and A. W. Rizzi, Solar wind flow past nonmagnetic planets—Venus and Mars, *Planet. Space Sci., 18,* 1281, 1970.
Taylor. H. A., Jr., H. C. Brinton, S. J. Bauer, R. E. Hartle, T. M. Donahue, P. A. Cloutier, R. C. Michel, R. E. Daniell, Jr., and B. H. Blackwell, Ionosphere of Venus: First observations of the dayside ion composition near dawn and dusk, *Science, 203,* 752, 1979*a*.
Taylor, H. A., Jr., H.C. Brinton, S. J. Bauer, R. E. Hartle, P. A. Cloutier, R. C. Michel, R. E. Daniell, Jr., T. M. Donahue, and R. C. Maehl, Ionosphere of Venus: First observations of the effects of dynamics on the dayside ion composition, *Science, 203,* 755, 1979*b*.
Vaisberg, O. L., S. A. Romanov, V. N. Smirnov, I. P. Karpinsky, B. I. Khazanov, B. V. Polenov, A. V. Bogdanov, and N. M. Antonov, Ion flux parameters in the solar wind-Venus interaction region according to the Venera 9 and Venera 10 data, in *Physics of Solar Planetary Environments,* edited by D. J. Williams, p. 904, AGU, Washington, D. C., 1976.
Wallis, M. K., Comet-like interaction of Venus with the solar wind. *Cosmic Electrodyn., 3,* 45, 1972.
Wolfe, J., D. S. Intriligator, J. Mihalov, H. Collard, D. McKibbin, R. Whitten, and A. Barnes, Initial observations of the Pioneer Venus orbiter solar wind plasma experiment, *Science, 203,* 750, 1979.
Wolff, R. S., B. E. Goldstein, and S. Kumar, A model of the variability of the Venus ionopause altitude, *Geophys. Res. Lett., 6,* 353, 1979.
Zwan, B. Y., and R. A. Wolf, Depletion of solar wind plasma near a planetary boundary, *J. Geophys. Res., 81,* 1636, 1976.

(Received March 5, 1980;
revised July 3, 1980;
accepted July 3, 1980.)